J. metamorphic Geol., 2007, **25,** 975–989 doi:10.1111/j.1525-1314.2007.00739.x

Ultrahigh-pressure eclogite transformed from mafic granulite in the Dabie orogen, east-central China

Y.-C. LIU,[1,2] S.-G. LI,[1] X.-F. GU,[1] S.-T. XU[3] AND G.-B. CHEN[4]
[1]*CAS Key Laboratory of Crust-Mantle Materials and Environments, School of Earth and Space Sciences, University of Science and Technology of China, Hefei 230026, China (liuyc@ustc.edu.cn)*
[2]*Beijing SHRIMP Center, Chinese Academy of Geological Sciences, Beijing 100037, China*
[3]*Anhui Institute of Geology, Hefei 230001, China*
[4]*Anhui Institute of Paleontology, Hefei 230001, China*

ABSTRACT Although ultrahigh-pressure (UHP) metamorphic rocks are present in many collisional orogenic belts, almost all exposed UHP metamorphic rocks are subducted upper or felsic lower continental crust with minor mafic boudins. Eclogites formed by subduction of mafic lower continental crust have not been identified yet. Here an eclogite occurrence that formed during subduction of the mafic lower continental crust in the Dabie orogen, east-central China is reported. At least four generations of metamorphic mineral assemblages can be discerned: (i) hypersthene + plagioclase ± garnet; (ii) omphacite + garnet + rutile + quartz; (iii) symplectite stage of garnet + diopside + hypersthene + ilmenite + plagioclase; (iv) amphibole + plagioclase + magnetite, which correspond to four metamorphic stages: (a) an early granulite facies, (b) eclogite facies, (c) retrograde metamorphism of high-pressure granulite facies and (d) retrograde metamorphism of amphibolite facies. Mineral inclusion assemblages and cathodoluminescence images show that zircon is characterized by distinctive domains of core and a thin overgrowth rim. The zircon core domains are classified into two types: the first is igneous with clear oscillatory zonation ± apatite and quartz inclusions; and the second is metamorphic containing a granulite facies mineral assemblage of garnet, hypersthene and plagioclase (andesine). The zircon rims contain garnet, omphacite and rutile inclusions, indicating a metamorphic overgrowth at eclogite facies. The almost identical ages of the two types of core domains (magmatic = 791 ± 9 Ma and granulite facies metamorphic zircon = 794 ± 10 Ma), and the Triassic age (212 ± 10 Ma) of eclogitic facies metamorphic overgrowth zircon rim are interpreted as indicating that the protolith of the eclogite is mafic granulite that originated from underplating of mantle-derived magma onto the base of continental crust during the Neoproterozoic (*c.* 800 Ma) and then subducted during the Triassic, experiencing UHP eclogite facies metamorphism at mantle depths. The new finding has two-fold significance: (i) voluminous mafic lower continental crust can increase the average density of subducted continental lithosphere, thus promoting its deep subduction; (ii) because of the current absence of mafic lower continental crust in the Dabie orogen, delamination or recycling of subducted mafic lower continental crust can be inferred as the geochemical cause for the mantle heterogeneity and the unusually evolved crustal composition.

Key words: Dabie orogen; eclogite; mafic lower continental crust; magma underplating.

INTRODUCTION

The Dabie-Sulu ultrahigh pressure (UHP) metamorphic belt in east-central China is one of the largest UHP terranes in the world (Xu *et al.*, 1994, 2005; Wang *et al.*, 1995; Cong, 1996; Zheng *et al.*, 2003). It was formed by continental collision between the South China Block (SCB) and North China Block in the Triassic (e.g. Li *et al.*, 1993, 1994, 2000; Rowley *et al.*, 1997; Hacker *et al.*, 1998; Ayers *et al.*, 2002; Liu *et al.*, 2005, 2007). It is well documented that the UHP rocks (e.g. coesite- and microdiamond-bearing eclogites) exhumed to the surface came from subducted upper and/or felsic lower continental crust with mafic boudins (e.g. Tabata *et al.*, 1998; Liou, 1999; Carswell *et al.*, 2000; Ernst, 2001; Li *et al.*, 2003a; Liu *et al.*, 2007). However, UHP eclogites formed by subduction of mafic lower continental crust have not been reported yet. Moreover, a geophysical study indicates the current absence of mafic lower continental crust in the Dabie-Sulu orogenic belt (Gao *et al.*, 1998). Therefore, it is an interesting question as to whether voluminous mafic lower crust was involved in continental subduction in the Dabie orogen. This question is important for understanding the average density of the subducted continental lithosphere and the extent of delamination or recycling of subducted mafic lower continental crust in the Dabie orogen. Here we report petrological and

© 2007 Blackwell Publishing Ltd

geochronological observations from the UHP eclogite formed by subduction of mafic lower continental crust in the Dabie orogen, China. These eclogites provide direct windows into the formation and evolution of the subducted mafic lower continental crust of the SCB.

GEOLOGICAL SETTING

It is generally accepted that the Dabie orogen can be divided into five major lithotectonic units from north to south (e.g. Okay, 1993; Li *et al.*, 2001, 2004; Xu *et al.*, 2003, 2005; Liu *et al.*, 2005, 2007; Zheng *et al.*, 2005; and references therein): (1) the Beihuaiyang zone; (2) the North Dabie high-*T*/UHP complex zone (NDZ); (3) the Central Dabie middle-*T*/UHP metamorphic zone (CDZ); (4) the South Dabie low-*T* eclogite zone (SDZ); (5) the Susong complex zone. These five zones are separated by the respective Xiaotian-Mozitan, Wuhe-Shuihou, Hualiangting-Mituo and Taihu-Mamiao faults (see Fig. 1). Zone (1) is composed of a fore arc flysch formation of the Foziling Group (Xu *et al.*, 1992a; Li *et al.*, 2001) and unsubducted continental crust of the Luzhenguan complex (Okay & Sengör, 1993; Zheng *et al.*, 2004; Jiang *et al.*, 2005). Zones (2), (3), (4) and (5) belong to the subducted SCB.

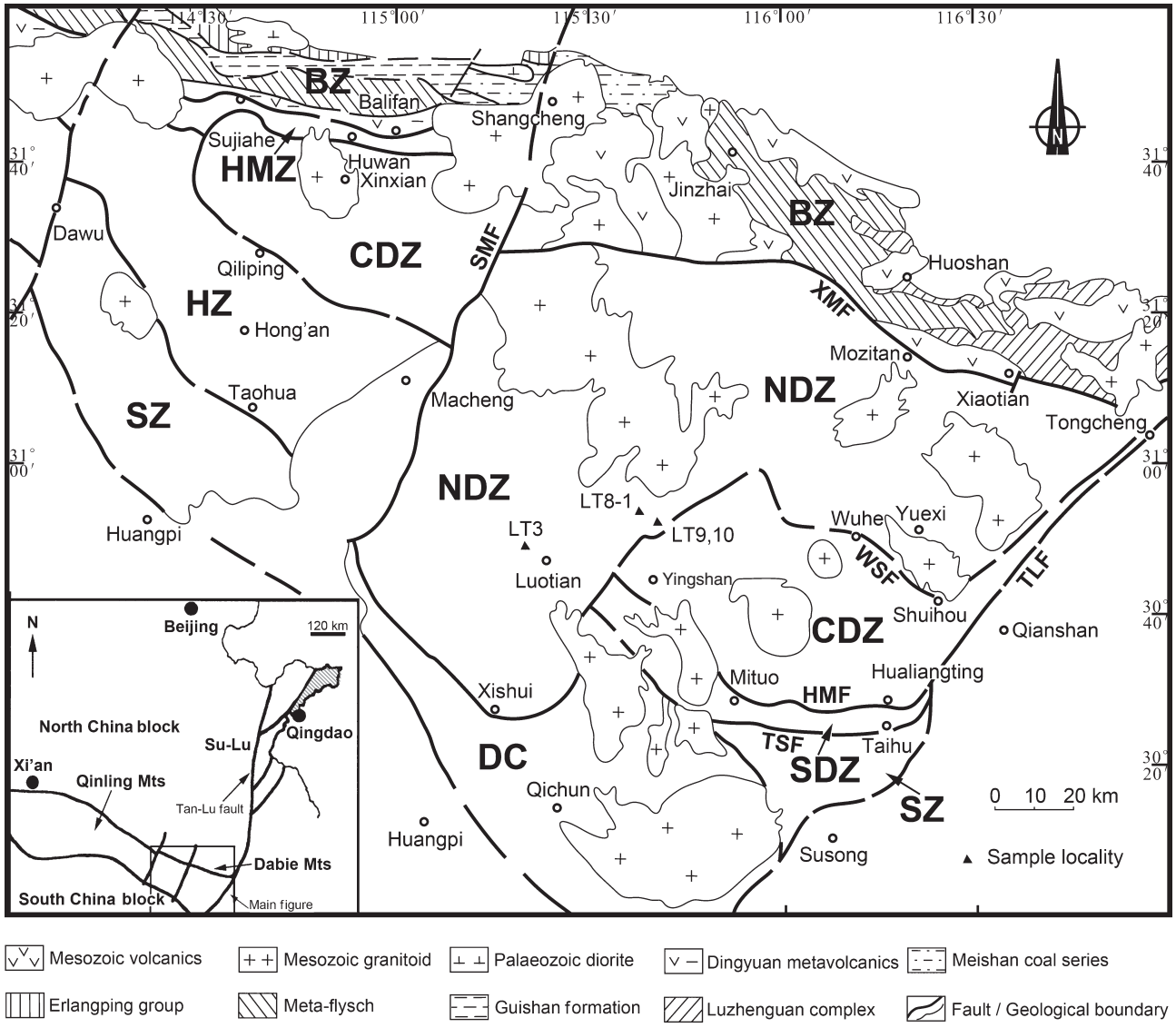

Fig. 1. Schematic geological map of the Dabie orogen, with inset showing the location of this area within the Triassic Qinling–Dabie–Su-Lu collision orogen in central China. Sample localities with sample numbers are described in detail in the text. BZ, Beihuaiyang zone; NDZ, North Dabie high-*T*/UHP complex zone; CDZ, Central Dabie middle-*T*/UHP metamorphic zone; SDZ, South Dabie low-T eclogite zone; SZ, Susong complex zone; HMZ, Huwan mélange zone; HZ, Hong'an low-*T* eclogite facies zone; DC, amphibolite facies Dabie complex; XMF, Xiaotian-Mozitan fault; WSF, Wuhe-Shuihou fault; HMF, Hualiangting-Mituo fault; TMF, Taihu-Mamiao fault; TLF, Tan-Lu fault.

© 2007 Blackwell Publishing Ltd

The UHP metamorphic rocks, including coesite-bearing eclogite, UHP gneiss, quartz jadeitite and marble with eclogite nodules, are observed in the CDZ and SDZ (e.g. Xu *et al*., 1992b, 1994, 2005; Okay & Sengör, 1993; Wang *et al*., 1995; Li *et al*., 2004). The occurrence of diamond and coesite in the UHP rocks in the CDZ indicates the UHP metamorphism occurred at 700–850 °C and >2.8 GPa (e.g. Okay *et al*., 1989; Wang *et al*., 1989; Xu *et al*., 1992b; Okay, 1993; Rolfo *et al*., 2000), whereas the peak *P–T* conditions on the eclogites in the SDZ were estimated at 670 °C and 3.3 GPa (Li *et al*., 2004). Wang *et al*. (1992) and Okay (1993) called the SDZ and CDZ units 'cold' and 'hot' eclogite terranes respectively. Both the CDZ and SDZ units sequentially experienced UHP eclogite facies and HP amphibolite facies retrograde metamorphism (e.g. Xu *et al*., 1992b; Wang *et al*., 1995; Cong, 1996; Li *et al*., 2004).

The NDZ is composed mainly of banded tonalitic and granitoid gneiss and post-collisional magma intrusions with minor meta-peridotite (including dunite, harzburgite and lherzolite), garnet pyroxenite, garnet-bearing amphibolite, granulite and eclogite. The oriented mineral exsolutions in garnet and clinopyroxene, and micro-diamond imply that the eclogites from the NDZ also underwent UHP metamorphism (Xu *et al*., 2003, 2005; Malaspina *et al*., 2006) at a possible pressure of >3.5–4.0 GPa. The Triassic zircon U–Pb (Liu *et al*., 2000) and Sm–Nd (Liu *et al*., 2005) ages of the eclogites from the NDZ suggest that they also formed by subduction of the SCB in the Triassic. The metamorphic ages (Liu *et al*., 2000, 2007; Bryant *et al*., 2004; Xie *et al*., 2004) and UHP metamorphic evidence (Liu *et al*., 2007) from the banded gneisses in the NDZ suggest that the gneisses surrounding the eclogites were also involved in the Triassic deep subduction of the SCB. Following the UHP eclogite facies metamorphism, however, the eclogites from the NDZ were first subjected to granulite facies retrogression, and later to amphibolite facies overprinting (e.g. Xu *et al*., 2000; Liu *et al*., 2001, 2005). This is distinctly different from the UHP rocks in the CDZ where there is only amphibolite facies retrogression (e.g. Okay, 1993; Wang *et al*., 1995; Cong, 1996). Therefore, although both the CDZ and NDZ units experienced UHP metamorphism, they had different exhumation histories, suggesting that the CDZ and NDZ are two decoupled UHP slabs (Liu *et al*., 2001, 2003, 2005, 2007; Zheng *et al*., 2001; Li *et al*., 2005). Pb isotope investigations show that the UHP rocks from the CDZ are characterized by high radiogenic Pb, but banded gneiss from the NDZ is characterized by low radiogenic Pb (Zhang *et al*., 2001; Li *et al*., 2003a). This suggests that the exhumed UHP rocks in the CDZ were from subducted upper crust, while the UHP rocks from the NDZ were from subducted lower felsic continental crust (Li *et al*., 2003a). It is also supported by their different lithological associations and peak hydrous mineral assemblages and metamorphic temperatures of the three eclogite-bearing slices in the Dabie UHP metamorphic belt (cf. Liu *et al*., 2007; and references therein). Fluid inclusions in the UHP rocks from the CDZ and NDZ are also different. The inclusions in the UHP rocks from the CDZ are mainly aqueous fluid with various salinities, while those in the UHP rocks from the NDZ are mainly N_2 or CO_2, suggesting more aqueous fluids in the CDZ during metamorphism (Xiao *et al*., 2001, 2002). These further indicate that their protoliths come from different crustal levels (e.g. upper and lower continental crust, respectively), probably resulted from the variable crustal depths of decoupling during subduction (Okay & Sengör, 1993; Liu *et al*., 2006, 2007).

The Luotian dome in the western segment of the NDZ is a deeply eroded area with abundant felsic and mafic granulites (Fig. 1). An unusual eclogite, with granulite facies mineral relics and later overprinting of granulite facies (see below in detail), was found as lenses in garnet-bearing banded tonalitic gneisses from the Luotian dome (see Fig. 1). Samples were collected from Jinjiapu (LT8-1, LT9 & LT10) and Sanlifan (LT3) (Fig. 1). Fresh eclogites are preserved in the core of these lenses or blocks, but there is retrogression into symplectite eclogite or garnet-bearing amphibolite from the centre towards the edge of the lens.

PETROGRAPHY

The mineral assemblage of eclogite from the Luotian dome is garnet, omphacite, and rutile with secondary minerals of quartz, diopside, hypersthene, hornblende, plagioclase and ilmenite (Fig. 2). The compositions of representative minerals from the samples are listed in Tables 1 and 2. The most striking feature of the eclogite is the presence of two generations of hypersthene and three generations of plagioclase. The first generation of hypersthene and plagioclase occurs as inclusions in porphyroblastic garnet (Fig. 2e) or in the core domain of zircon. This plagioclase (mostly andesine with An = 33–47 mol.% and minor labradorite with An = 58 mol.%) (Table 1) also occurs as the only inclusion in the core of porphyroblastic garnet (Fig. 2f). The second generation of hypersthene occurs as a symplectite associated with diopside and plagioclase, or the retrograded rim of Na-clinopyroxene with quartz exsolution (Fig. 2c–e). The third generation of plagioclase, which is albitic (compositionally ranging from oligoclase to andesine) with An = 27–45 mol.%, occurs as symplectite associated with hornblende, that resulted from the breakdown of garnet (Fig. 2a,e), or with clinopyroxene (omphacite or diopside) (Fig. 2c). The mineral inclusions of plagioclase (andesine) ± hypersthene in the core of porphyroblastic garnet are relic minerals of the eclogite precursor whereas eclogitic facies minerals inclusions – such as omphacite and rutile – occur in the mantle of porphyroblastic garnet (Fig. 2a,b,f). Most garnet has no obvious zoning,

© 2007 Blackwell Publishing Ltd

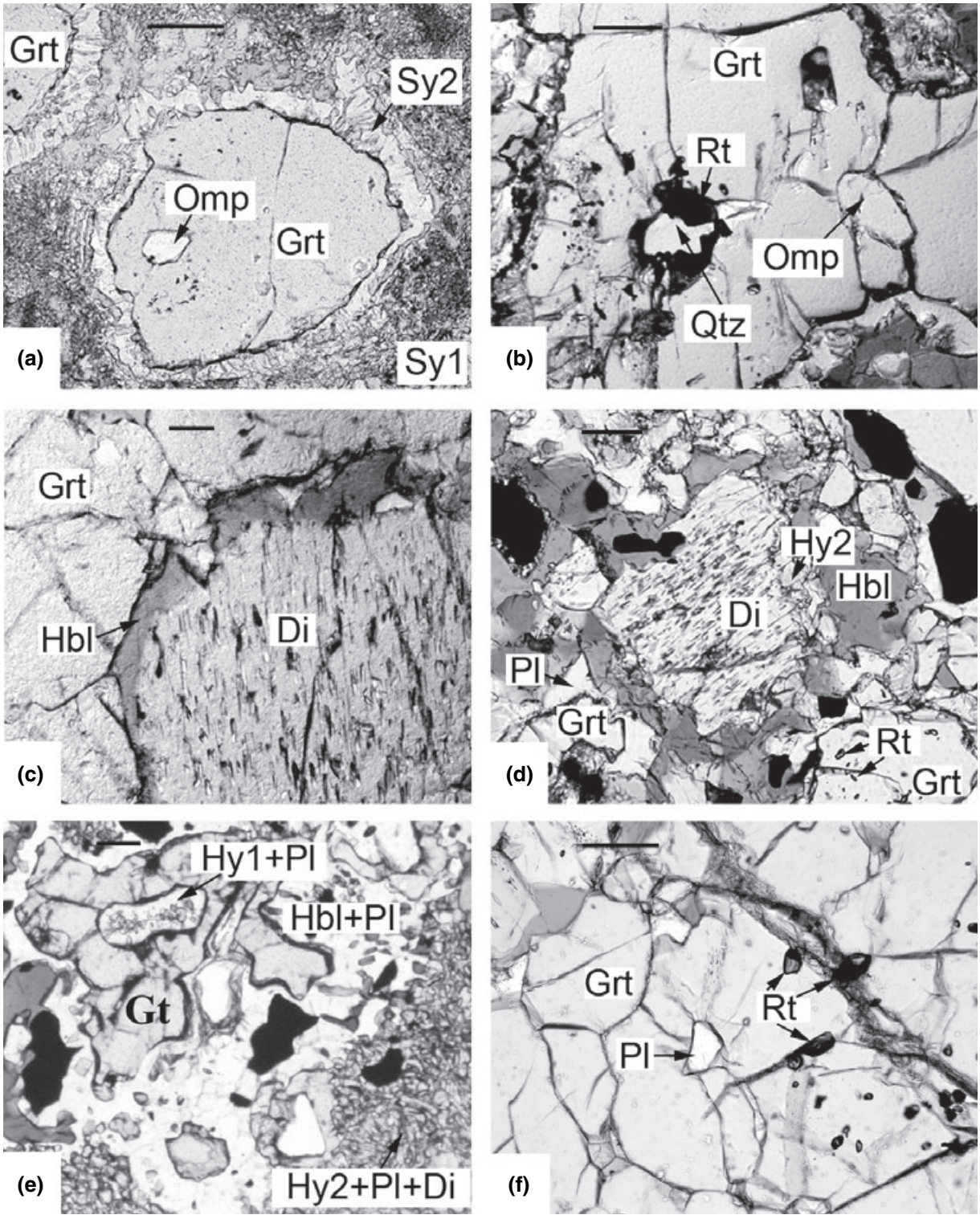

Fig. 2. Photomicrographs of eclogite from the Luotian dome in the Dabie orogen. (a) Omphacite inclusion in garnet with two generations of symplectites (Sy1 & Sy2), sample LT10; (b) Omphacite, rutile and quartz inclusions in garnet, sample LT8-1. (c) Diopside with quartz needles contains retrogressed hornblende margin, sample LT8-1. (d) Diopside with quartz needles contains retrograded hypersthene margin, sample LT8-1. (e) Hypersthene and plagioclase inclusions in garnet, sample LT3. (f) Porphyroblastic garnet contains plagioclase and rutile inclusions in the core and mantle, respectively, sample LT8-1. Hy1, first-generation hypersthene; Hy2, second-generation hypersthene; Sy1, earlier granulite facies symplectite composed of plagioclase, diopside and hypersthene; Sy2, later amphibolite facies symplectite composed of plagiosclase and hornblende. Mineral abbreviations are after Kretz (1983). The scale bar is 100 μm.

© 2007 Blackwell Publishing Ltd

Table 1. Electron microprobe analyses of representative minerals from the eclogites in the Luotian dome.

Mineral	Garnet		Omphacite		Diopside		Hypersthene			Hornblende		Plagioclase		
No.	LT8-1	LT9	LT10	LT8-1	LT8-1	LT10	LT10	LT9	LT9	LT10	LT9	LT8-1	LT8-1	LT10
Locality	m	m	i	i	m	Sy1	Sy1	i	Sy1	Sy2	Sy2	i	Sy2	Sy1
SiO_2	39.51	39.95	56.75	54.13	52.82	54.24	54.9	52.31	52.42	46.59	45.65	57.12	60.37	56.67
TiO_2	0.01	0	0	0.17	0	0.02	0	0	0	0.47	0.98	0	0	0
Al_2O_3	22.26	21.79	0.1	6.65	3.65	2.15	0.68	0.61	0.69	12.21	9.36	26.9	24.47	25.66
FeO	22.08	21.82	3.26	5.64	5.93	5.47	19.21	30.02	29.27	8.1	16.55	0.42	0.12	0.6
Cr_2O_3	0	0	0	0	0	0.1	0	0	0	0.2	0	0.03	0	0
MnO	0.31	0.23	0	0	0	0.05	0.3	0.28	0.26	0.11	0.06	0	0	0.02
MgO	8.35	5.26	9.61	12	14.41	14.43	23.72	16.15	16.7	14.97	10.27	0	0	0.92
CaO	7.47	10.74	13.76	19.28	22.04	23.28	0.52	0.61	0.64	12.1	11.31	9.17	5.75	10.26
Na_2O	0	0	6.5	2.69	1.13	0.76	0	0	0	2.04	1.63	6.35	8.68	6.43
K_2O	0	0	0	0	0	0	0	0	0	0.09	0	0	0	0
Total	99.99	99.99	99.98	100.56	99.98	99.99	99.33	99.98	99.98	96.68	95.81	99.99	99.39	100.56
O	12	12	6	6	6	6	6	6	6	23	23	8	8	8
Si	3.01	3.08	2.01	1.96	1.93	1.99	2.03	2.03	2.03	6.71	6.89	2.57	2.703	2.549
Al^{IV}	0	0	0	0.04	0.07	0.01	0	0	0	1.29	1.11	1.42	1.29	1.359
Al^{VI}	2	1.98	0.42	0.24	0.09	0.09	0.03	0.03	0.03	0.78	0.56			
Fe^{3+}	0.07	0.01	0.01	0	0.06	0	0	0	0	0.08	0.15	0	0	0
Ti	0	0	0	0.01	0	0	0	0	0	0.05	0.11	0	0	0
Fe^{2+}	1.34	1.34	0.09	0.17	0.12	0.17	0.59	0.97	0.95	0.9	1.94	0.02	0.004	0.023
Cr	0	0	0	0	0	0	0	0	0	0.02	0	0	0	0
Mg	0.95	0.6	0.51	0.65	0.79	0.79	1.31	0.93	0.96	3.21	2.31	0	0	0.062
Mn	0.02	0.02	0	0	0	0	0.01	0.01	0.01	0.01	0.09	0	0	0.001
Ca	0.61	0.9	0.52	0.75	0.86	0.9	0.02	0.02	0.03	1.87	1.83	0.44	0.276	0.495
Na	0	0	0.45	0.19	0.08	0.05	0	0	0	0.57	0.48	0.55	0.754	0.561
K	0	0	0	0	0	0	0	0	0	0.02	0	0	0	0

m, matrix; i, inclusion in garnet; sy1 and sy2 denote symplectites of granulite facies and amphibolite facies retro-metamorphism respectively. Garnet/pyroxene stoichiometries and the amount of Fe^{3+} and Fe^{2+} were estimated based on eight/four cations and the charge-balance constraint; the ferric iron content in amphibole was calculated as Si + Al + Ti + Mg + Fe + Mn = 13 for O = 23.

Table 2. Electron microprobe analyses of representative minerals in zircon and a weak zoned garnet porphyroblast from the eclogites in the Luotian dome.

Mineral	Garnet					Omphacite		Hypersthene	Plagioclase	
Spot no.	LT10	LT9	LT10	LT10	LT10	LT9	LT10	LT10	LT10Pl	LT9
Locality	Zir-C	Zir-C	M-C	M-M	M-R	Zir-R	Zir-R	Zir-C	Zir-C	Zir-C
SiO_2	40.78	38.68	41.51	40.84	41.36	54.51	56.76	53.93	56.73	55.58
TiO_2	0	0	0	0	0	0.07	0.04	0	0	0.01
Al_2O_3	22.97	21.14	22.78	22.95	23.11	9.13	9.49	0.72	27.44	28.3
FeO	18.88	24.57	17.24	17.17	17.87	7.14	1.89	21.15	0.02	0.02
Cr_2O_3	0.01	0.02	0	0	0	0	0.07	0.01	0	0.01
MnO	0.57	1.91	0.26	0.55	0.49	0.06	0.03	0.5	0	0
MgO	10.28	3.06	11.07	10.86	10.33	9.2	10.59	23.94	0	0
CaO	6.48	10.18	7.22	8.27	7.55	15.13	15.06	0.38	9.77	11.48
Na_2O	0	0.02	0	0.02	0	4.75	5.84	0.04	5.96	4.47
K_2O	0	0	0	0	0	0	0	0	0.05	0.06
Total	99.97	99.61	100.08	100.66	100.71	99.99	99.77	100.67	99.97	99.93
O	12	12	12	12	12	6	6	6	8	8
Si	3.07	3.05	3.1	3.03	3.08	1.97	2.01	1.98	2.55	2.5
Al^{IV}	0	0	0	0	0	0.03	0	0.02	1.45	1.5
Al^{VI}	2.03	1.97	2	2.01	2.03	0.36	0.4	0.01		
Fe^{3+}	0.06	0.08	0.05	0.05	0.06	0	0	0.02	0	0
Ti	0	0	0	0	0	0	0	0	0	0
Fe^{2+}	1.13	1.54	1.02	1.01	1.06	0.22	0.06	0.63	0	0
Cr	0	0	0	0	0	0	0	0	0	0
Mg	1.15	0.36	1.23	1.2	1.15	0.5	0.56	1.31	0	0
Mn	0.04	0.13	0.02	0.03	0.03	0	0	0.02	0	0
Ca	0.52	0.86	0.58	0.66	0.6	0.59	0.57	0.01	0.47	0.55
Na	0	0	0	0	0	0.33	0.4	0	0.52	0.39
K	0	0	0	0	0	0	0	0	0	0
Grs	15.53	25.75	17.66	20.02	18.56					
Alm	39.73	53.27	35.9	34.8	37.26					
Prp	40.6	12.45	43.25	41.3	40.42					
Sps	1.28	4.41	0.58	1.19	1.09					
Adr	2.83	3.95	2.61	2.58	2.67					
Jd						33.88	40.31	0.1		
An									47.4	58.5

M-C, M-M and M-R denote the core, mantle and rim domains of a garnet porphyroblast in the matrix respectively. Zir-C and Zir-R represent the core and rim domains of zircon respectively. Garnet/pyroxene stoichiometries and the amount of Fe^{3+} and Fe^{2+} were estimated based on eight/four cations and the charge-balance constraint.

© 2007 Blackwell Publishing Ltd

which may be ascribed to fast exhumation and/or high-*T* overprinting of the eclogites. Rare garnet porphyroblasts show weak zoning from core, mantle to rim involving the variation of grossular components from 17.66, 20.02 to 18.56 mol.%, respectively (Table 2). Furthermore, plagioclase and omphacite inclusions commonly occur in the core and mantle domains of larger porphyroblastic garnet (Fig. 2a,f) respectively. This weak zoning and distribution of inclusion phases indicate the possibility that some garnet cores preserve evidence of an early, granulite facies equilibrium condition. Similarly, the mantle of this zoned garnet possibly represents the peak UHP conditions. It therefore seems very likely that the compositional zoning of garnet reflects the variation of pressure conditions relating to an evolution from early granulite to eclogite and later granulite facies overprinting as described later in detail. In addition, the hypersthene coexisting with andesine occurs as inclusions in the core domain of zircon (see below in detail). Cathodoluminescene (CL) and back-scatter electron images show that the Neoproterozoic metamorphic zircon core domains with both hypersthene and andesine inclusions of granulite facies have no fractures (Fig. 3h) and some of them contain an overgrowth rim with eclogitic minerals (see latter in detail), which rules out the later or exotic origin of mineral inclusions in the zircon core. Consequently, the precursor of the eclogite was mafic granulite.

As with other diamond-bearing eclogites in the NDZ (Xu *et al.*, 2003, 2005; Liu *et al.*, 2005), the corona structures of the garnet from the eclogites are characterized by double symplectites. There is an inner corona composed of fine-grained amphibole and plagioclase derived from the decomposition of garnet during amphibolite facies retrogression, while the outer corona is a very narrow zone between garnet and clinopyroxene or omphacite composed of very fine-grained minerals (e.g. hypersthene, diopside and plagioclase), which was formed by retrogressive reaction between garnet and clinopyroxene under granulite facies conditions (Fig. 2a,e) (Liu *et al.*, 2005). Vermicular symplectites indicate retrogressive reaction or decompression breakdown during fast exhumation. In addition, the peak assemblage in these rocks is garnet + omphacite + rutile ± diamond with no hydrous minerals (e.g. phengite) (Xu *et al.*, 2003, 2005), indicating that an anhydrous paragenesis formed at dry conditions. Therefore, the absence of fluid during their peak and initial retrograde metamorphic conditions may be related to the nature of its protolith, i.e. 'dry' mafic lower crustal rock (mafic granulite) as mentioned above.

Although no diamond or coesite has been found in the samples, the eclogites have metamorphic evolutional histories and petrographic characteristics similar to the diamond-bearing eclogites or UHP mafic rocks in the NDZ (Xu *et al.*, 2005; Malaspina *et al.*, 2006). For example, a spectacular microstructure of oriented quartz needles in matrix Ca–Na clinopyroxene is widespread (Fig. 2c,d) and is evidence for the prior existence of a 'supersilicic' omphacite stabilized at UHP conditions (≥2.5 GPa) (Tsai & Liou, 2000). Thus, it is reasonable to infer that the eclogites also underwent UHP metamorphism. On the basis of microstructural observations and mineral relationships as mentioned above, at least four generations of mineral assemblages for the eclogites can be discerned: (i) hypersthene + plagioclase ± garnet; (ii) omphacite + garnet + rutile + quartz; (iii) symplectite stage of garnet + diopside + hypersthene + ilmenite + plagioclase; (iv) amphibole + plagioclase + magnetite. Based on the major element compositions of paragenetic minerals, metamorphic *P–T* conditions for the four metamorphic stages of the eclogite in the Luotian dome are estimated as follows (Table 3): (i) granulite facies stage at ~0.8 GPa; (ii) eclogite facies stage at ~2.5 GPa and 853–880 °C, averaging 864 °C; (iii) retrograde metamorphism of high-pressure granulite facies stage at 1.1–1.4 GPa and 804–857 °C; (iv) retrograde metamorphism of amphibolite facies at 0.5–0.7 GPa and 706–777 °C. In view of the new finding of microdiamond from the eclogite (Xu *et al.*, 2003, 2005) and enclosing orthogneiss (Liu *et al.*, 2007) in the NDZ, the peak metamorphic conditions were reestimated at 900–960 °C (averaging 930 °C) at 4.0 GPa, corresponding to the lowest pressure for diamond formation (Xu *et al.*, 1992b).

ZIRCON U–Pb GEOCHRONOLOGY

Analytical methods

Zircon was separated from ~5 kg of each sample by crushing and sieving, followed by magnetic and heavy liquid separation and hand-picking under binoculars. Approximately 500 zircon grains for each sample, together with a zircon U–Pb standard TEM (417 Ma), were mounted using epoxy, which was then polished until all zircon grains were approximately cut in half. The internal zoning patterns of the crystals were observed by CL image, which was analysed at the Institute of Mineral Resources, Chinese Academy of Geological Sciences (CAGS).

Zircon from the eclogites was dated on a SHRIMP II at Beijing SHRIMP Center. Uncertainties in ages are quoted at the 95% confidence level (2σ). Spot diameter was 30 μm for SHRIMP II. Common Pb corrections were made using measured ^{204}Pb. The SHRIMP analyses followed the procedures as described by Williams (1998). Both optical photomicrographs and CL images were taken as a guide to selection of U–Pb dating spot. Five scans through the mass stations were made for each age determination. Standards used were SL13, with an age of 572 Ma and U content of 238 p.p.m., and TEM, with an age of 417 Ma (Williams, 1998; Black *et al.*, 2003). The U–Pb isotope data were treated following Compston *et al.*

© 2007 Blackwell Publishing Ltd

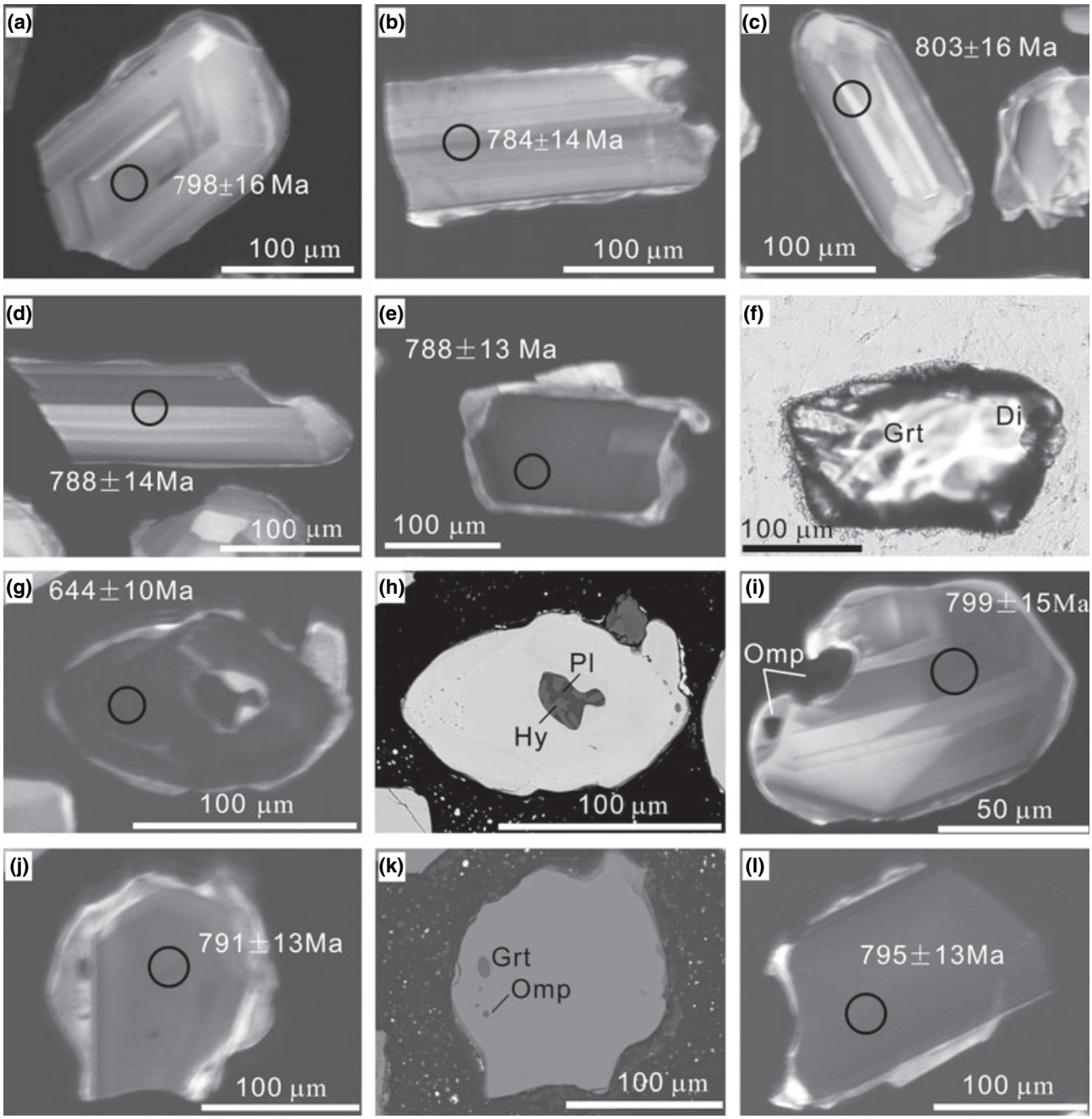

Fig. 3. Cathodoluminescene (CL) images (a–e, g, i, j and l), back-scatter electron (BSE) pictures (h and k), and plane-polarized light (PL) photo (f) for zircon from sample LT10. Zircon (e) and (f), (g) and (h), and (j) and (k) are the same grain. The open circles are analysis spots with available $^{206}Pb/^{238}U$ ages. Hy, hypersthene; other mineral abbreviations are the same as those in Fig. 2.

(1992) with the ISOPLOT program of Ludwig (2001). Our measurement of standard zircon TEMORA 1 yielded a weighted $^{206}Pb/^{238}U$ age of 416.9 ± 3.5Ma (MSWD = 2, $n = 20$), which is in good agreement with the recommended isotope dilution-thermal ionization mass spectrometry age of 416.75 ± 0.24 Ma (Black *et al.*, 2003).

Mineral inclusions in zircon have been used to characterize zircon origin. Mineral inclusions were identified using Raman spectroscopy at the Analytical Centre, China University of Geosciences (Wuhan) and the Continental Dynamics Laboratory, CAGS, and/or substantiated using the electron microprobe analyser (EMPA) at the Analytical Centre, China University of Geosciences (Wuhan) and the Institute of Mineral Resources, CAGS. The analytical conditions on the Raman and EMPA were in accordance with that reported by Xu *et al.* (2005) and Liu *et al.* (2005).

© 2007 Blackwell Publishing Ltd

Table 3. *P–T* estimates of the eclogites from the Luotian dome, NDZ.

Metamorphic facies	Temperature (°C)			Pressure (GPa)
Earlier granulite				Garnet-hypersthene 0.8 (Wood, 1974)
Eclogite	Garnet-omphacite			
	K	RH	EG	
	853	860	880	2.5
	904	963	927	4
Later granulite	Diopside-hypersthene			Garnet-hypersthene
	W	WB		Wood (1974)
	804	813		1.4
	857	849		1.1
Amphibolite	Plagioclase-amphibole			Al in amphibole
	BH			BH, JR, S
	706–777			0.5–0.7

K, Krogh (1988); RH, Raheim & Green (1974); EG, Ellis & Green (1979); W, Wells (1977); WB, Wood & Banno (1973); BH, Blundy & Holland (1990); JR, Johnson & Rutherford (1988); S, Schmidt (1992). The amphibolite facies pressures are inferred from the Al content in amphibole of the symplectites after omphacite or garnet (Schmidt, 1992), though these values must be taken with caution, they are similar to those from the country rocks (granitoid gneiss) and garnet-bearing amphibolites in the NDZ (Zhang *et al*., 1996).

The representative CL images for the studied samples are presented in Figs 3 & 4. The compositions of representative mineral inclusions in zircon are reported in Table 2. The U–Pb data for zircon dating are listed in Tables 4 & 5.

Mineral inclusions diagnostic of zircon origin

A powerful means of linking zircon growth/recrystallization to metamorphic events is by integrated CL imaging and mineral inclusion assemblage within different domains of a zircon grain (e.g. Gebauer *et al*., 1997; Hermann *et al*., 2001; Liu *et al*., 2004). Zircon from samples LT10 and LT9 is granular, platy and prismatic with diameters of 100–300 μm (Figs 3 & 4). Mineral inclusions in zircon were identified by electron microprobe (Table 2) and Raman spectroscopy (Fig. 5). Most zircon shows typical core and rim textures in CL image. Inherited zircon cores can be divided into two types. One has grey or light grey core with clear oscillatory zonation and is surrounded by a relatively strong-luminescent rim (Figs 3a–d & 4a,b) and the second is black or deep grey, unzoned, with a weak-luminescent and surrounded by strong-luminescent rim (Figs 3e,f,i,j,l & 4c,d,f,h). The first type usually contains apatite (Figs 4a & 5f) and quartz minerals or no mineral inclusion and the second type contains a mineral assemblage of granulite facies, such as garnet, hypersthene and plagioclase (andesine) (Figs 3e–h, 4f & 5a). Therefore, these two styles of zircon cores represent a magmatic and granulite facies metamorphic origin respectively. In addition, some zircon rims contain garnet and/or omphacite or rutile inclusions (Figs 3i–k, 4e,g & 5b–d), indicating that the metamorphic overgrowth formed during eclogite facies

Table 4. SHRIMP zircon U–Pb data for eclogite (sample LT10) from the Luotian dome.

Spot	Domain	Inclusion in domain	$^{206}Pb_c$ %	U (p.p.m.)	Th (p.p.m.)	Th/U	$^{206}Pb^*$ (p.p.m.)	$^{207}Pb^*/^{206}Pb^*$	± %	$^{207}Pb^*/^{235}U$	± %	$^{206}Pb^*/^{238}U$	± %	$^{206}Pb/^{238}U$ age (Ma)
LT10-1.1	me, c	Gt	0.26	393	582	1.48	44.1	0.0671	1.4	1.204	2.2	0.1301	1.7	788 ± 13
LT10-1.2	me, c	No	0.7	276	520	1.88	30.1	0.0645	2.9	1.122	3.5	0.1262	1.8	766 ± 13
LT10-2.1	ma, c	No	0.57	193	277	1.43	21.6	0.0656	2.5	1.167	3.1	0.1291	1.8	783 ± 13
LT10-2.2	ma, c	No	1.28	87	103	1.18	9.16	0.0636	5.6	1.062	6	0.1211	2.1	737 ± 15
LT10-4.1	ma, c	No	0.36	240	149	0.62	21.5	0.0641	2.6	0.919	3.2	0.104	1.9	638 ± 11
LT10-3.1	ma, c	No	0.6	224	326	1.45	25.8	0.0653	2.8	1.201	3.3	0.1334	1.9	807 ± 14
LT10-3.2	me, c	No	0.75	79	85	1.07	9.34	0.067	2.8	1.256	3.5	0.136	2.2	822 ± 17
LT10-4.2	ma, c	No	0.47	195	328	1.68	21.9	0.0696	3.9	1.248	4.4	0.13	1.9	788 ± 14
LT10-3.3	me, c	No	2.81	44	40	0.91	5.25	0.0608	14	1.12	15	0.1338	3.6	810 ± 27
LT10-3.4	me, c	No	0.28	64	48	0.75	7.46	0.0733	4.2	1.37	4.8	0.1356	2.3	820 ± 18
LT10-1.4	me, c	Gt + Omp in rim	0.23	373	525	1.41	42	0.0693	1.8	1.247	2.5	0.1305	1.8	791 ± 13
LT10-4.3	me, c	Hy	0.96	375	369	0.98	17.4	0.0614	4.4	0.452	4.9	0.0534	2.1	335 ± 7
LT10-1.3	me, c	No	0.54	347	413	1.19	37.1	0.0669	2.4	1.143	3	0.1239	1.8	753 ± 13
LT10-3.5	ma, c	Omp in rim	0.41	184	155	0.84	20.9	0.0678	3.5	1.234	4	0.1319	1.9	799 ± 15
LT10-3.6	me, c	Hy, Pl	0.66	134	94	0.7	13.2	0.068	4.1	1.069	4.6	0.114	2.1	696 ± 14
LT10-3.7	me, c	No	1.71	91	61	0.67	9.52	0.0662	9.1	1.09	9.4	0.1193	2.3	726 ± 15
LT10-3.8	ma, c	No	1.07	165	202	1.22	16.8	0.0734	3.1	1.19	3.7	0.1176	2	717 ± 14
LT10-3.9	ma, c	No	0.58	70	43	0.61	6.33	0.0729	6	1.053	6.5	0.1047	2.3	642 ± 14
LT10-4.4	ma, c	No	0.56	226	182	0.8	25.2	0.0655	2.9	1.168	3.7	0.1292	2.2	784 ± 16
LT10-4.5	ma, c	No	0.96	107	152	1.42	12.3	0.0681	2.8	1.238	3.5	0.1319	2.1	798 ± 16
LT10-1.5	me, c	No	0.42	244	431	1.77	28.3	0.0667	2.5	1.239	3.1	0.1347	1.8	815 ± 14
LT10-4.7	ma, c	No	0.4	191	193	1.01	21.5	0.0684	2.2	1.231	3.1	0.1305	2.1	791 ± 16
LT10-1.6	me, c	No	0.38	326	896	2.75	36.9	0.0656	1.9	1.188	2.6	0.1313	1.8	795 ± 13
LT10-1.7	me, c	No	0.4	351	669	1.9	39.3	0.0637	3	1.14	3.5	0.1299	1.8	787 ± 14
LT10-4.6	ma, c	No	1.23	164	324	1.97	18.3	0.0702	4.1	1.242	4.5	0.1284	1.9	779 ± 14
LT10-4.8	ma, c	No	0.34	161	269	1.67	18	0.0656	2.2	1.169	2.9	0.1294	1.9	784 ± 14
LT10-4.9	ma, c	No	0	80	94	1.17	9.08	0.0711	2.4	1.3	3.2	0.1326	2.1	803 ± 16
LT10-1.8	me, c	No	0.27	464	687	1.48	51.6	0.06656	1.4	1.185	2.3	0.1292	1.8	783 ± 13
LT10-1.9	me, c	No	0.78	408	559	1.37	42.4	0.0655	2.3	1.083	3	0.1199	1.8	730 ± 12
LT10-1.10	me, c	Hy, Pl	0.3	1491	1994	1.34	135	0.06647	1	0.962	2	0.105	1.7	644 ± 10
LT10-1.11	me, c	No	0.63	264	381	1.44	30.2	0.0662	2.6	1.206	3.2	0.132	1.9	799 ± 14
LT10-1.12	me, c	No	0.15	297	700	2.36	33.3	0.0694	1.8	1.246	2.6	0.1303	1.8	790 ± 14

Pb_c and Pb* indicate the common and radiogenic portions respectively. Pb*: corrected for common ^{204}Pb using measured ^{204}Pb. All errors are 1σ. Mineral abbreviations are the same as those in Figs 2 & 3. me, metamorphic zircon; ma, magmatic zircon with oscillatory growth zonation; c, core.

© 2007 Blackwell Publishing Ltd

Table 5. SHRIMP zircon U–Pb data for eclogite (sample LT9) from the Luotian dome.

Spot	Domain	Inclusion in domain	$^{206}Pb_c$ %	U (p.p.m.)	Th (p.p.m.)	Th/U	$^{206}Pb^*$(p.p.m.)	$^{207}Pb^*/^{206}Pb^*$	± %	$^{207}Pb^*/^{235}U$	± %	$^{206}Pb^*/^{238}U$	± %	$^{206}Pb/^{238}U$ Age (Ma)
LT9-1-1.1	me, c	No	0.1	2446	659	0.27	107	0.058	1.6	0.4078	2.3	0.051	1.7	321 ± 6
LT9-1-2.1	ma, c	Ap	1.2	156	254	1.63	18	0.0625	4.2	1.143	4.7	0.1325	2.2	802 ± 16
LT9-1-3.1	me, c	Gt	0.96	73	48	0.66	8.73	0.0778	4.3	1.474	4.9	0.1374	2.3	830 ± 18
LT9-1-4.1	me, r	Gt in core	10.23	59	1	0.01	1.9	0.045	71	0.21	71	0.0334	4.7	212 ± 10
LT9-1-4.2	me, c	No	0.75	215	24	0.11	10	0.0669	6.9	0.499	7.1	0.0541	1.9	339 ± 6
LT9-1-4.3	me, c	No	2	148	34	0.23	11.4	0.0569	8.3	0.692	8.5	0.0882	2.1	545 ± 11
LT9-1-1.2	me, c	No	0.47	924	712	0.77	103	0.06759	1.3	1.202	2.2	0.129	1.7	782 ± 13
LT9-1-4.4	me, c	No	0.22	789	357	0.45	73.8	0.06507	1.3	0.975	2.2	0.1086	1.8	665 ± 11
LT9-1-2.2	ma, c	No	0.24	227	249	1.1	23.6	0.065	2.2	1.083	3	0.1209	2.1	736 ± 14
LT9-1-1.3	me, c	No	0.1	967	1069	1.1	94.7	0.06099	1.5	0.957	2.3	0.1138	1.8	695 ± 12
LT9-1-1.4	me, c	No	0.25	1018	2266	2.22	103	0.0647	1.8	1.05	2.5	0.1177	1.8	717 ± 12
LT9-1-1.5	me, c	No	0.08	659	673	1.02	69.2	0.0644	1.9	1.084	2.6	0.1221	1.8	743 ± 13
LT9-1-1.6	me, c	No	0.21	1885	463	0.24	97.1	0.05832	1.2	0.481	2.1	0.0598	1.7	375 ± 6
LT9-1-3.3	me, r	omp	7.1	85	0	0	2.5	0.043	37	0.187	37	0.0318	3.3	202 ± 7
LT9-1-1.7	me, c	No	0.26	482	931	1.93	48.1	0.064	1.6	1.023	2.4	0.1159	1.8	707 ± 12

Pb_c and Pb* indicate the common and radiogenic portions respectively. Pb*: corrected for common ^{204}Pb using measured ^{204}Pb. All errors are 1σ. Mineral abbreviations are after Kretz (1983). me, metamorphic zircon; ma, magmatic zircon with oscillatory growth zonation; r, overgrowth rim; c, core.

conditions. These observations also suggest that there was an earlier metamorphic stage of granulite facies prior to the eclogite facies metamorphism in the eclogites, which is consistent with the petrographic observations described above. It is worth noting that only a few zircon grains have a thin metamorphic overgrowth rim and most grains do not. This may indicate the absence of fluid during the eclogite facies metamorphism, because the dissolution and overgrowth of zircon depend on the availability of fluids during HP metamorphism (e.g. Williams *et al.*, 1996; Rubatto *et al.*, 1999; Liermann *et al.*, 2002; Zheng *et al.*, 2004; Wu *et al.*, 2006). The absence of fluid during the eclogite facies metamorphism is ascribed to the protolith nature of the mafic lower crust, which is in agreement with the above petrographic observations such as the absence of hydrous minerals in the peak stage.

SHRIMP zircon U–Pb dating results

A total of 32 U–Pb spot analyses were made on 30 zircon from LT10 (Table 4; Fig. 6a). The magmatic and granulite facies metamorphic zircon cores from sample LT10 record $^{206}Pb/^{238}U$ concordant ages ranging from 807 to 783 Ma and from 822 to 766 Ma (mostly 810–783 Ma), respectively, which yield weighted mean ages of 791 ± 9 Ma with MSWD of 0.44 ($n = 10$) and 794 ± 10 Ma with MSWD of 1.2 ($n = 12$) (Fig. 6a,c,d). The high Th/U ratio (0.67–2.75) of the metamorphic zircon cores (Table 4) is attributed to their granulite facies metamorphic origin, because such zircon has high Th/U ratios (e.g. Vavra *et al.* 1999), in contrast to UHP metamorphic zircon. It is also supported by the hypersthene + plagioclase ± garnet inclusion assemblage within the metamorphic zircon core domains mentioned above. The 15 analyses of the cores of magmatic and metamorphic zircon from sample LT9 define a discordia line with an upper intercept age of 778 ± 78 Ma and a lower intercept age of 210 ± 88 Ma (MSWD = 2.9) (Fig. 6b). This lower intercept age is consistent with a concordant age of 212 ± 10 Ma given by a metamorphic overgrowth zircon rim with a Th/U ratio of 0.01, which contains eclogitic minerals such as omphacite, garnet and rutile (Figs 3i–k, 4e,g & 5b–d), suggesting it is the result of the Triassic eclogite facies metamorphism. Consequently, the eclogites within the Luotian dome were transformed from Neoproterozoic mafic granulite by deep subduction of the continental crust of the SCB in the Triassic.

IMPLICATIONS FOR RECYCLING OF SUBDUCTED CONTINENTAL CRUST

The almost identical ages of the Neoproterozoic granulite facies metamorphic and magmatic zircon from the studied eclogites (794 ± 10 and 791 ± 9 Ma respectively) imply that the precursor of the eclogite originated from Neoproterozoic basic magma underplating on the base of continental crust in the northern margin of the SCB. This is supported by the Neoproterozoic crustal growth event in the SCB. It is well known that there was large-scale magmatic activity during the middle Neoproterozoic in the SCB, especially in the periphery of the SCB (e.g. Rowley *et al.*, 1997; Li *et al.*, 1999, 2003b,c; Zheng *et al.*, 2004), which was interpreted as being related to plume activity and breakup of the supercontinent Rodinia. Furthermore, $\varepsilon_{Nd}(t)$ values and Nd model ages (T_{DM}) for Proterozoic to Permian sedimentary rocks in the SCB show a sharp change with a significant increase in $\varepsilon_{Nd}(t)$ but a decrease in T_{DM} at *c.* 820–750 Ma (Li & McCulloch, 1996). This Nd isotope change suggests a large increase in the proportion of juvenile mantle-derived materials from the provenance of the SCB during the Rodinia breakup, which caused the mafic lower continental crust overgrowth in the SCB formed by underplating of the Neoproterozoic mantle-derived magma. Therefore, after the Neoproterozoic,

© 2007 Blackwell Publishing Ltd

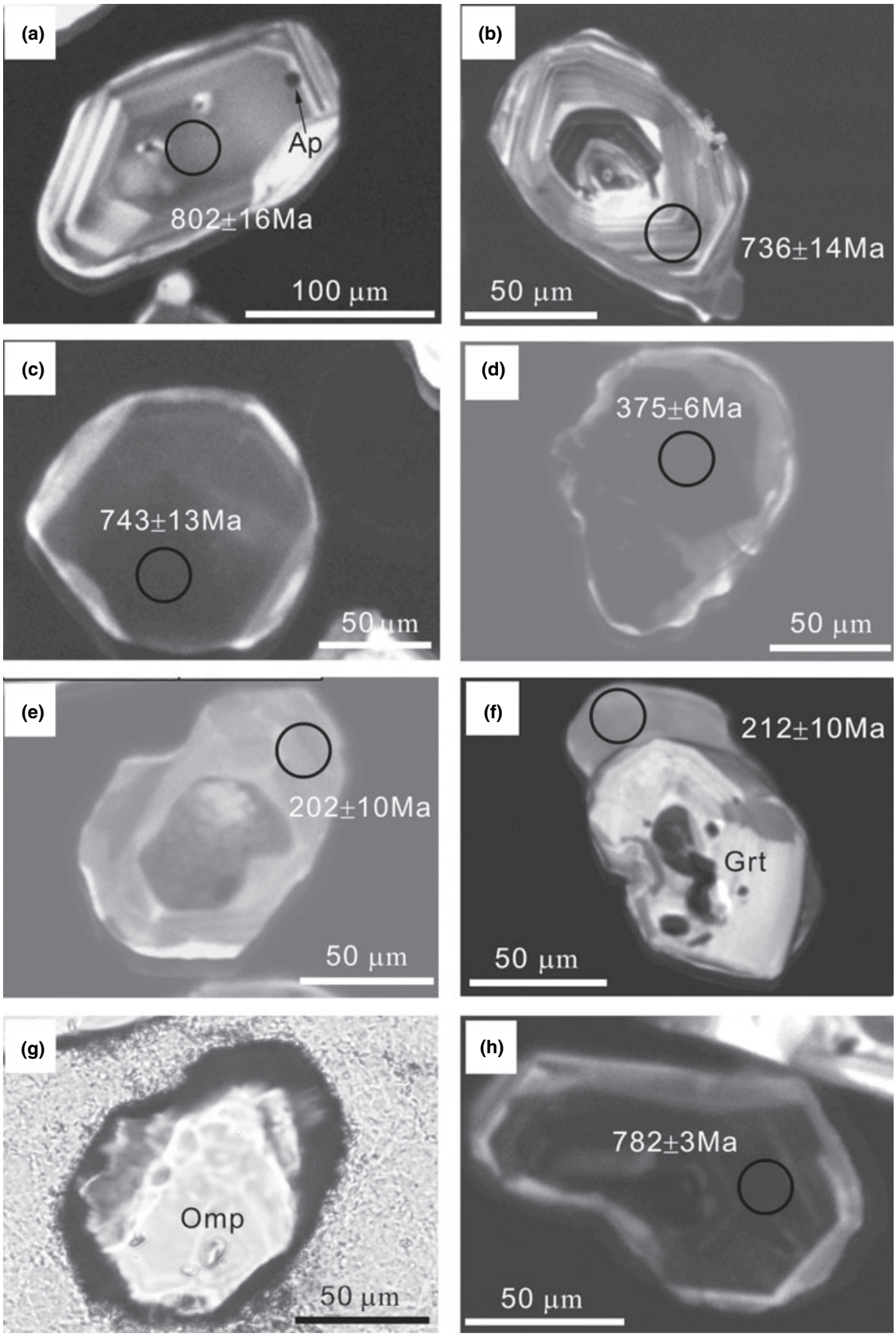

© 2007 Blackwell Publishing Ltd

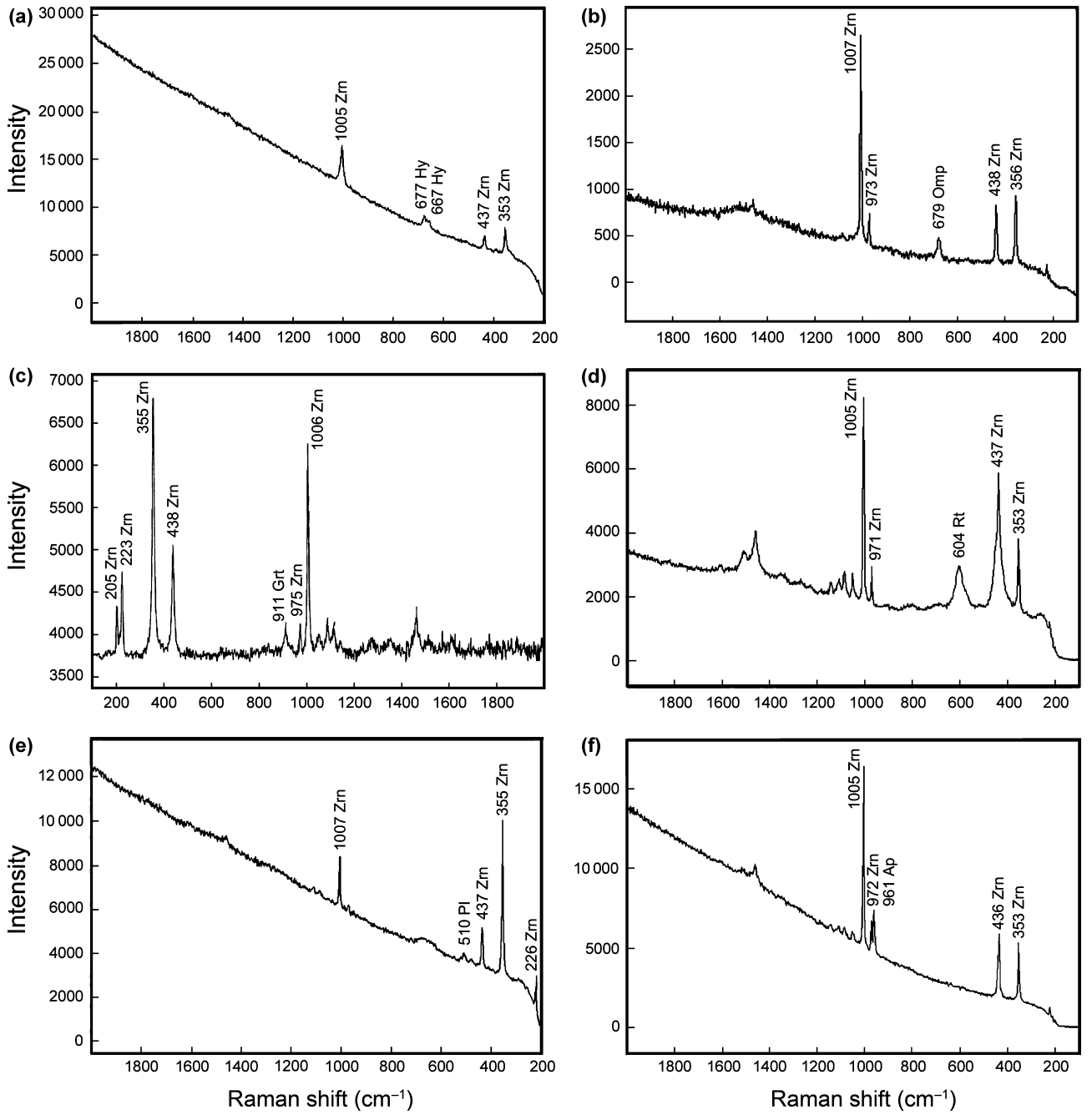

Fig. 5. Representative Raman spectra of mineral inclusions in zircon of eclogites from the Luotian dome. (a) Hypersthene. (b) Omphacite. (c) Garnet. (d) Rutile. (e) Plagioclase. (f) Apatite. These spectra also contain host zircon peaks at 205, 223–226, 353–356, 436–438, 971–975 and 1005–1007 cm^{-1}.

the continental lithosphere of the SCB should have a greater proportion of mafic lower continental crust and a relatively higher average density than before. In addition, early Cretaceous adakitic rocks reported in the Dabie orogen (Wang *et al.*, 2007; Xu *et al.*, 2007), which were produced by partial melting of the thickened mafic lower continental crust underneath the Dabie orogen, document that the thickened mafic lower continental crust remained until the collapse of the Dabie orogen in the early Cretaceous. This new

Fig. 4. Cathodoluminescene (CL) images (a–f and h) and plane-polarized light (PL) photograph (g) for zircon from sample LT9. Zircon (e) and (g) are the same grain. The analysis spot marked with open circle and its $^{206}Pb/^{238}U$ age is shown in each grain. Mineral abbreviations are after Kretz (1983).

© 2007 Blackwell Publishing Ltd

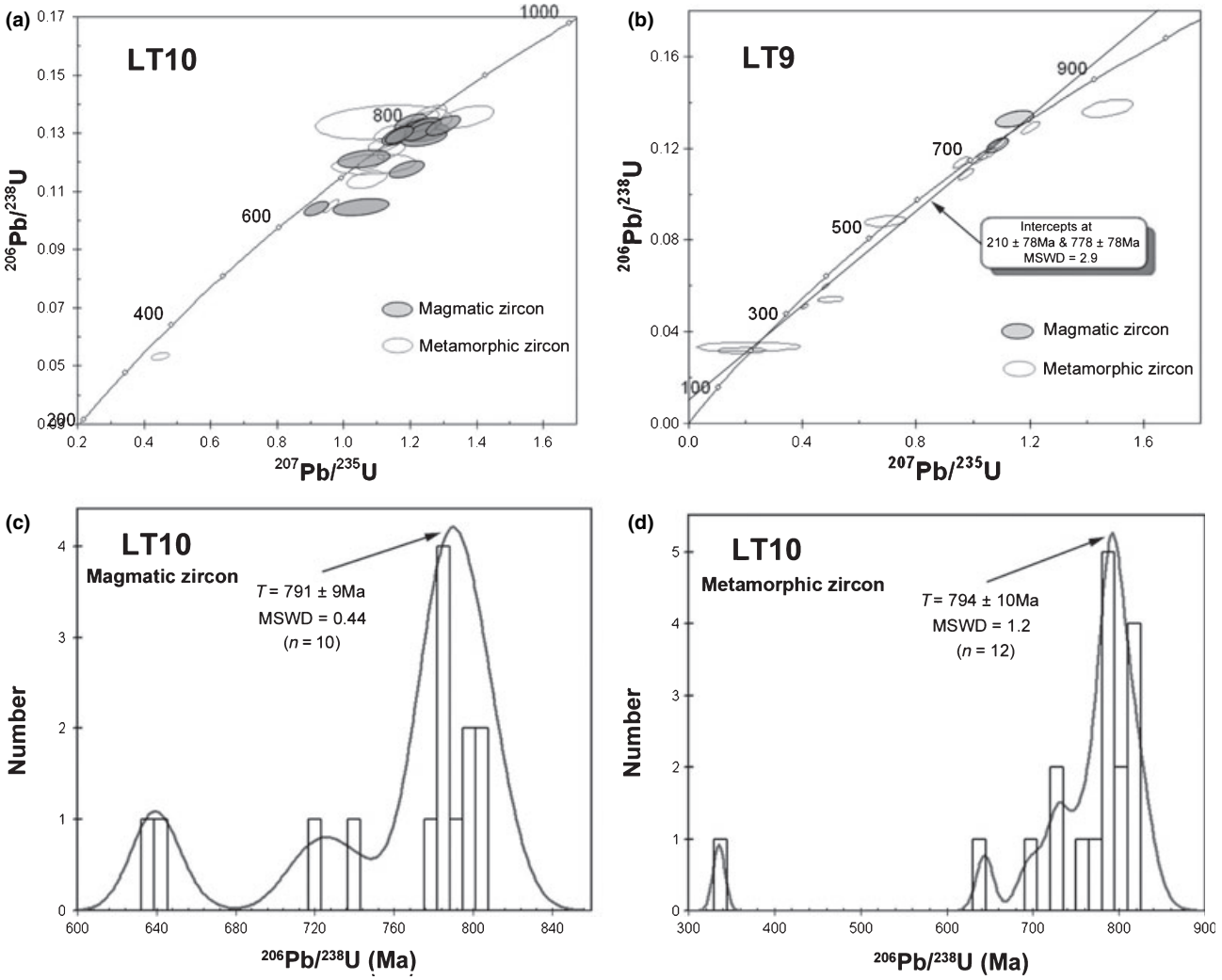

Fig. 6. Zircon SHRIMP U–Pb dating for eclogites (samples LT10 and LT9) from the Luotian dome. (a) and (b) show concordia plots for zircon from samples LT10 and Lt9 respectively. (c) and (d) show histograms of apparent $^{206}Pb/^{238}U$ of all analyses of inherited cores of magmatic and metamorphic zircon from sample LT10 with peaks at 791 and 794 Ma, respectively.

occurrence of the Triassic eclogite, transformed from Neoproterozoic mafic granulite, indicates that the mafic lower continental crust formed by the Neoproterozoic basic magma underplating was involved in the Triassic continental subduction. The relatively higher average density of the subducting continental crust of the SCB may have promoted the deep subduction of the SCB in the Triassic.

Although the subducted mafic lower continental crust of the SCB could have been thick in the Triassic, geophysical investigation shows that the mafic lower continental rocks in the Dabie orogen or even in the northern margin of the SCB are scarce at present. It can be reasonably deduced that the subducted mafic lower continental crust may be delaminated and recycled into the underlying convective mantle, which could be a means of explaining the mantle heterogeneity and the evolved chemical composition of the continental crust (e.g. Kay & Kay, 1991; Rudnick, 1995; and references therein).

ACKNOWLEDGEMENTS

This research was financially supported by the National Natural Science Foundation of China (40572035 and 40634023), the Major State Research Program of China (G1999075503) and the Chinese National Key Project for Basic Research (2003 CB716500). We thank D. Liu, Y. Wang and H. Tao for their help in SHRIMP U–Pb dating on zircon, Z. Chen for the CL image, M. He and L. Yan for the Raman analysis, and H. Liu and Z. Chen for electron microprobe analysis. Y. Zheng and F. Huang are thanked for their suggestions on earlier versions of this manuscript, which helped clarify some

© 2007 Blackwell Publishing Ltd

ambiguities as well as the English presentation. D. Robinson, D. Nakamura and J. C. Ayers are thanked for the critical review of the manuscript and for many useful suggestions.

REFERENCES

Ayers, J. C., Dunkle, S., Gao, S. & Miller, C. F., 2002. Constraints on timing of peak and retrograde metamorphism in the Dabie Shan ultrahigh-pressure metamorphic belt, east–central China, using U–Th–Pb dating of zircon and monazite. *Chemical Geology*, **186,** 315–331.

Black, L. P., Kamo, S. L., Allen, C. M. *et al.*, 2003. TEMORA 1: a new zircon standard for Phanerozoic U-Pb geochronology. *Chemical Geology*, **200,** 155–170.

Blundy, J. D. & Holland, T. J. B., 1990. Calcic amphibole equilibria and a new amphibole-plagioclase geothermometer. *Contributions to Mineralogy and Petrology*, **104,** 208–224.

Bryant, J. L., Ayers, J. C., Gao, S., Miller, C. F. & Zhang, H., 2004. Geochemical, age, and isotopic constrains on the location of the Sino-Korean/Yangtze suture and evolution of the Northern Dabie Complex, east central China. *Geological Society of America Bulletin*, **116,** 698–717.

Carswell, D. A., Wilson, R. N. & Zhai, M., 2000. Metamorphic evolution, mineral chemistry and thermobarometry of schists and orthogneisses hosting ultra-high pressure eclogites in the Dabieshan of central China. *Lithos*, **52,** 121–155.

Compston, W., Williams, I. S., Kirschvink, J. L., Zhang, Z. & Ma, G., 1992. Zircon U–Pb ages for the early Cambrian timescale. *Journal of the Geological Society (London)*, **149,** 171–184.

Cong, B., 1996. *Ultrahigh-Pressure Metamorphic Rocks in the Dabieshan-Sulu Region of China*. Science Press, Beijing, 224 pp.

Ellis, D. J. & Green, D. H., 1979. An experimental study of the effect of Ca upon garnet-clinopyroxene Fe-Mg exchange equilibration. *Contributions to Mineralogy and Petrology*, **71,** 13–22.

Ernst, W. G., 2001. Subduction, ultrahigh-pressure metamorphism, and regurgitation of buoyant crustal slices – implications for arcs and continental growth. *Physics of the Earth and Planetary Interiors*, **127,** 253–275.

Gao, S., Zhang, B., Jin, Z., Kern, H., Luo, T. & Zhao, Z., 1998. How mafic is the lower continental crust? *Earth and Planetary Science Letters*, **161,** 101–117.

Gebauer, D., Schertl, H.-P., Brix, M. & Schreyer, W., 1997. 35 Ma old ultrahigh-pressure metamorphism and evidence for very rapid exhumation in the Dora Maira Massif, Western Alps. *Lithos*, **41,** 5–24.

Hacker, B. R., Ratschbacher, L., Webb, L. E., Ireland, T. R., Walker, D. & Dong, S., 1998. U/Pb zircon ages constrain the architecture of the ultrahigh-pressure Qinling-Dabie orogen, China. *Earth and Planetary Science Letters*, **161,** 215–230.

Hermann, J., Rubatto, D., Korsakov, A. & Shatsky, V. S., 2001. Multiple zircon growth during fast exhumation of diamondiferous, deeply subducted continental crust (Kokchetav massif, Kazakhstan). *Contributions to Mineralogy and Petrology*, **141,** 66–82.

Jiang, L., Wolfgang, S., Chen, F., Liu, Y.-C. & Chu, D., 2005. U-Pb zircon ages for the Luzhenguan Complex in northern part of the eastern Dabie orogen. *Science in China (Series D)*, **48,** 1357–1367.

Johnson, M. C. & Rutherford, M. J., 1988. Experimental calibration of an aluminum-in-hornblende geobarometer applicable to calcalkaline rocks. *EOS*, **69,** 1511.

Kay, R. W. & Kay, S. M., 1991. Creation and destruction of lower continental crust. *Geologische Rundschau*, **80,** 259–278.

Kretz, R., 1983. Symbols for rock-forming mineral. *American Mineralogist*, **68,** 277–279.

Krogh, E. J., 1988. The garnet-clinopyroxene Fe-Mg geothermometer – a reinterpretation of existing experimental data. *Contributions to Mineralogy and Petrology*, **99,** 44–48.

Li, X. & McCulloch, M. T., 1996, Secular variation in Nd isotopic composition of Neoproterozoic sediments from the southern margin of the Yangtze Block: evidence for a Proterozoic continental collision in southern China. *Precambrian Research*, **76,** 67–76.

Li, S., Xiao, Y., Liu, D. *et al.*, 1993. Collision of the North China and Yangtze blocks and formation of coesite-bearing eclogites: timing and processes. *Chemical Geology*, **109,** 89–111.

Li, S., Wang, S., Chen, Y. *et al.*, 1994. Excess argon in phengite from eclogite: evidence from dating of eclogite minerals by Sm–Nd, Rb–Sr and $^{40}Ar/^{39}Ar$ method. *Chemical Geology*, **112,** 343–350.

Li, Z. X., Li, X. H., Kinny, P. D. & Wang, J., 1999. The breakup of Rodinia: did it start with a mantle plume beneath South China? *Earth and Planetary Science Letters*, **173,** 171–181.

Li, S., Jagoutz, E., Chen, Y. & Li, Q., 2000. Sm–Nd and Rb–Sr isotope chronology of ultrahigh-pressure metamorphic rocks and their country rocks at Shuanghe in the Dabie Mountains, central China. *Geochimica Cosmochimica Acta*, **64,** 1077–1093.

Li, S., Huang, F., Nie, Y. *et al.*, 2001. Geochemical and geochronological constrains on the suture location between the North and South China Blocks in the Dabie orogen, central China. *Physics and Chemistry of the Earth (A)*, **26,** 655–672.

Li, S., Huang, F., Zhou, H. & Li, H., 2003a. U-Pb isotopic compositions of the ultrahigh pressure metamorphic (UHPM) rocks from Shuanghe and gneisses from Northern Dabie zone in the Dabie Mountains, central China: constraint on the exhumation mechanism of UHPM rocks. *Science in China, Series D*, **46,** 200–209.

Li, X. H., Li, Z. X., Ge, W. *et al.*, 2003b. Neoproterozoic granitoids in South China: crustal melting above a mantle plume at ca. 825 Ma? *Precambrian Research*, **122,** 45–83.

Li, Z. X., Li, X. H., Kinny, P. D., Wang, J., Zhang, S. & Zhou, H., 2003c. Geochronology of Neoproterozoic syn-rift magmatism in the Yangtze Craton, South China and correlations with other continents: evidence for a mantle superplume that broke up Rodinia. *Precambrian Research*, **122,** 85–109.

Li, X.-P., Zheng, Y.-F., Wu, Y.-B., Chen, F. K., Gong, B. & Li, Y.-L., 2004. Low-T eclogite in the Dabie terrane of China: petrological and isotopic constrains on fluid activity and radiometric dating. *Contributions to Mineralogy and Petrology*, **148,** 443–470.

Li, S., Li, Q., Hou, Z., Yang, W. & Wang, Y., 2005. Cooling history and exhumation mechanism of the ultrahigh-pressure metamorphic rocks in the Dabie Mountains, central China. *Acta Petrologica Sinica*, **21,** 1117–1124 (in Chinese with English abstract).

Liermann, H.-P., Isachsen, C., Altenberger, U. & Oberhänsli, R., 2002. Behavior of zircon during high-pressure, low-temperature metamorphism: case study from the Internal Unit of the Seisia zone (western Italian Alps). *European Journal of Mineralogy*, **14,** 61–71.

Liou, J. G., 1999. Petrotectonic summary of less intensively studied UHP regions. *International Geology Review*, **41,** 571–586.

Liu, Y.-C., Li, S., Xu, S. *et al.*, 2000. U-Pb zircon ages of the eclogite and tonalitic gneiss from the northern Dabie Mountains, China and multi-overgrowths of metamorphic zircons. *Geological Journal of China Universities*, **6,** 417–423 (in Chinese with English abstract).

Liu, Y.-C., Xu, S., Li, S. *et al.*, 2001. Distribution and metamorphic P-T condition of the eclogites from the mafic-ultramafic belt in the northern part of the Dabie Mountains. *Acta Geologica Sinica*, **75,** 385–395 (in Chinese with English abstract).

Liu, Y.-C., Xu, S., Li, S., Jiang, L., Chen, G. & Wu, W., 2003. Tectonic affinity, T–t path and uplift trajectory of eclogites

© 2007 Blackwell Publishing Ltd

from northern Dabie Mountains, central-eastern China. *Journal of China University of Geosciences*, **14,** 28–33.
Liu, F. L., Xu, Z. Q., Liou, J. G. & Song, B., 2004. SHRIMP U-Pb ages of ultrahigh-pressure and retrograde metamorphism of gneisses, south-western Sulu terrane, eastern China. *Journal of Metamorphic Geology*, **22,** 315–326.
Liu, Y.-C., Li, S., Xu, S. *et al*., 2005. Geochemistry and geochronology of eclogites from the northern Dabie Mountains, central China. *Journal of Asian Earth Sciences*, **25,** 431–443.
Liu, Y.-C., Li, S., Gu, X. & Hou, Z., 2006. Zircon SHRIMP U-Pb dating for olivine gabbro at Wangmuguan in the Beihuaiyang zone and its geological significance. *Chinese Science Bulletin*, **51,** 2500–2506.
Liu, Y.-C, Li, S. & Xu, S., 2007. Zircon SHRIMP U-Pb dating for gneiss in northern Dabie high T/P metamorphic zone, central China: implication for decoupling within subducted continental crust. *Lithos*, **96,** 170–185.
Ludwig, K. R., 2001. *User's Manual for Isoplot/Ex (rev. 2.49): A Geochronological Toolkit for Microsoft Excel*. Special Publication, No. 1a. Berkeley Geochronology Center, Berkeley, CA, 55 pp.
Malaspina, N., Hermann, J., Scambelluri, M. & Compagnoni, R., 2006. Multistage metasomatism in ultrahigh-pressure mafic rocks from the North Dabie Complex (China). *Lithos*, **90,** 19–42.
Okay, A. I., 1993. Petrology of a diamond and coesite-bearing metamorphic terrain: Dabie Shan, China. *European Journal of Mineralogy*, **5,** 659–675.
Okay, A. I. & Sengör, A. M. C., 1993. Tectonics of an ultrahigh-pressure metamorphic terrane: the Dabie Shan/Tongbai orogen, China. *Tectonics*, **12,** 1320–1334.
Okay, A. I., Xu, S. & Sengör, A. M. C., 1989, Coesite from the Dabie Shan eclogites, central China. *European Journal of Mineralogy*, **1,** 595–598.
Raheim, A. & Green, D. H., 1974. Experimental determination of the temperature and pressure dependence of the Fe-Mg partition coefficient for coexisting garnet and clinopyroxene. *Contributions to Mineralogy and Petrology*, **48,** 179–203.
Rolfo, F., Compagnoni, R., Xu, S. & Jiang, L., 2000. First report of felsic whiteschist in the ultrahigh-pressure metamorphic belt of Dabie Shan, China. *European Journal of Mineralogy*, **12,** 883–898.
Rowley, D. B., Xue, F., Tucker, R. D., Peng, Z. X., Baker, J. & Davis, A., 1997. Ages of ultrahigh pressure metamorphism and protolith orthogneisses from the eastern Dabie Shan: U/Pb zircon geochronology. *Earth and Planetary Science Letters*, **151,** 191–203.
Rubatto, D., Gebauer, D. & Compagnoni, R., 1999. Dating of eclogite facies zircons: the age of Alpine metamorphism in the Sesia-Lanzo zone (western Alps). *Earth and Planetary Science Letters*, **167,** 141–158.
Rudnick, R. L., 1995. Making continental crust. *Nature*, **378,** 571–578.
Schmidt, M. W., 1992. Amphibole composition in tonalite as a function of pressure: an experimental calibration of the Al-in-hornblende barometer. *Contributions to Mineralogy and Petrology*, **110,** 304–310.
Tabata, H., Yamauchi, K., Maruyama, S. & Liou, J. G., 1998. Tracing the extent of a UHP metamorphic terrane: mineral-inclusion study of zircons in gneisses from the Dabie Shan. In: *When Continents Collide: Geodynamics and Geochemistry of Ultrahigh-Pressure Rocks* (eds Hacker, B.R. & Liou, J.G.), pp. 261–273. Kluwer Academic Publishers, Dordrecht.
Tsai, C.-H. & Liou, J.G., 2000. Eclogite facies relics and inferred ultrahigh-pressure metamorphism in the North Dabie complex, central China. *American Mineralogist*, **85,** 1–8.
Vavra, G., Schmid, R. & Gebauer, D., 1999. Internal morphology, habit and U–Th–Pb microanalysis of amphibolite-to-granulite facies zircons: geochronology of the Ivrea Zone (Southern Alps). *Contributions to Mineralogy and Petrology*, **134,** 380–404.
Wang, X., Liou, J. G. & Mao, H. K., 1989. Coesite-bearing eclogites from the Dabie Mountains in central China. *Geology*, **17,** 1085–1088.
Wang, X., Liou, J. G. & Maruyama, S., 1992. Coesite-bearing eclogites from the Dabie Mountains, central China: petrogenesis, P–T paths, and implication for regional tectonics. *The Journal of Geology*, **100,** 231–250.
Wang, X., Zhang, R. Y. & Liou, J. G., 1995. UHPM terrane in east central China. In: *Ultrahigh Pressure Metamorphism* (eds Coleman, R.G. & Wang, X.), pp. 356–390. Cambridge University Press, Cambridge.
Wang, Q., Wyman, D. A., Xu, J. *et al*., 2007. Early Cretaceous adakitic granites in the Northern Dabie Complex, central China: implications for partial melting and delamination of thickened lower crust. *Geochimica et Cosmochimica Acta*, **71,** 2609–2636.
Wells, R. A., 1977. Pyroxene thermometry in simple and complex systems. *Contributions to Mineralogy and Petrology*, **62,** 129–139.
Williams, I. S., 1998. U–Th–Pb geochronology by ion microprobe. *Reviews in Economic Geology*, **7,** 1–35.
Williams, I. S., Buick, I. S. & Cartwright, I., 1996. An extended episode of early Mesoproterozoic metamorphic fluid flow in the Reynolds Range, central Australia. *Journal of Metamorphic Geology*, **14,** 29–47.
Wood, B. J., 1974. The solubility of alumina in orthopyroxene coexisting with garnet. *Contributions to Mineralogy and Petrology*, **46,** 1–15.
Wood, B. J. & Banno, S., 1973. Garnet-orthopyroxene and orthopyroxene-clinopyroxene relationship in simple and complex systems. *Contributions to Mineralogy and Petrology*, **42,** 109–124.
Wu, Y.-B., Zheng, Y.-F., Zhao, Z.-F., Gong, B., Liu, X. M. & Wu, F.-Y., 2006. U-Pb, Hf and O isotope evidence for two episodes of fluid-assisted zircon growth in marble-hosted eclogites from the Dabie orogen. *Geochimica et Cosmochimica Acta*, **70,** 3743–3761.
Xiao, Y., Hoefs, J., van den Kerkhof, A. M. & Li, S., 2001. Geochemical constraints of the eclogite and granulite facies metamorphism as recognized in the Raobazhai complex from North Dabie Shan, China. *Journal of Metamorphic Geology*, **19,** 3–19.
Xiao, Y., Hoefs, J., van den Kerkhof, A. M., Simon, K., Fiebig, J. & Zheng, Y., 2002. Fluid history during HP and UHP metamorphism in Dabie Shan, China: constraints from mineral chemistry, fluid inclusions, and stable isotopes. *Journal of Petrology*, **43,** 1505–1527.
Xie, Z., Gao, T. & Chen, J., 2004. Multi-stage evolution of gneiss from North Dabie: evidence from zircon U-Pb chronology. *Chinese Science Bulletin*, **49,** 1963–1969.
Xu, S., Jiang, L., Liu, Y.-C. & Zhang, Y., 1992a. Tectonic framework and evolution of the Dabie Mountains in Anhui, eastern China. *Acta Geologica Sinica*, **5,** 221–238.
Xu, S., Okay, A. I., Ji, S. *et al*., 1992b. Diamond from the Dabie Shan metamorphic rocks and its implication for tectonic setting. *Science*, **256,** 80–82.
Xu, S., Liu, Y.-C., Jiang, L., Su, W. & Ji, S., 1994. *Tectonic Regime and Evolution of Dabie Mountains*. Science Press, Beijing, 175 pp.
Xu, S., Liu, Y.-C., Su, W., Wang, R., Jiang, L. & Wu, W., 2000. Discovery of the eclogite and its petrography in the Northern Dabie Mountain. *Chinese Science Bulletin*, **45,** 273–278.
Xu, S., Liu, Y.-C., Chen, G. *et al*., 2003. New finding of microdiamonds in eclogites from Dabie-Sulu region in central-eastern China. *Chinese Science Bulletin*, **48,** 988–994.
Xu, S., Liu, Y.-C., Chen, G., Ji, S., Ni, P. & Xiao, W., 2005. Microdiamonds, their classification and tectonic implications for the host eclogites from the Dabie and Su-Lu regions in central eastern China. *Mineralogical Magazine*, **69,** 509–520.
Xu, H., Ma, C. & Ye, K., 2007. Early cretaceous granitoids and their implications for the collapse of the Dabie orogen, eastern

© 2007 Blackwell Publishing Ltd

China: SHRIMP zircon U–Pb dating and geochemistry. *Chemical Geology*, **240,** 238–259.

Zhang, R. Y., Liou, J. G. & Tsai, C. H., 1996. Petrogenesis of a high-temperature metamorphic terrane: a new tectonic interpretation for the north Dabieshan, central China. *Journal of Metamorphic Geology*, **14,** 319–333.

Zhang, H., Gao, S., Zhang, B., Zhong, Z., Jia, W. & Wang, L., 2001. Pb isotopic study on crustal structure of Dabie Mountains, central China. *Geochimica*, **30,** 395–401 (in Chinese with English abstract).

Zheng, Y., Fu, B., Li, Y. L., Wei, C. & Zhou, J., 2001. Oxygen isotope composition of granulites from Dabieshan in eastern China and its implications for geodynamics of Yangtze plate subduction. *Physics and Chemistry of the Earth (A)*, **26,** 673–684.

Zheng, Y., Fu, B., Gong, B. & Li, L., 2003. Stable isotope geochemistry of ultrahigh pressure metamorphic rocks from the Dabie-Sulu orogen in China: implications for geodynamics and fluid regime. *Earth Science Reviews*, **62,** 105–161.

Zheng, Y., Wu, Y., Chen, F., Gong, B., Li, L. & Zhao, Z., 2004. Zircon U-Pb and oxygen isotope evidence for a large-scale ^{18}O depletion event in igneous rocks during the Neoproterozoic. *Geochimica et Cosmochimica Acta*, **68,** 4145–4165.

Zheng, Y.-F., Zhou, J.-B., Wu, Y.-B. & Zhao, Z.-F., 2005. Low-grade metamorphic rocks in the Dabie-Sulu orogenic belt: a passive-margin accretionary wedge deformed during continent subduction. *Internal Geology Review*, **47,** 851–871.

Received 17 December 2006; revision accepted 1 August 2007.

© 2007 Blackwell Publishing Ltd